Progress in large-eddy simulation of premixed and partially-premixed turbulent combustion

By L. Duchamp de Lageneste AND H. Pitsch

1. Motivation and objectives

In many practical devices such as gas turbines and internal combustion engines, liquid fuel is injected as a spray and mixed with oxidizer as it vaporizes, so that combustion takes place in a partially-premixed regime. While partially-premixed flame propagation has been the subject of extensive experimental investigations (Su 2000; Muniz & Mungal 1997), its numerical simulation remains a challenging task. The mechanisms by which turbulence, chemical reactions, and heat release interact are still under investigation. Results by Veynante (1994) suggest the importance of premixed flame propagation in the process of flame stabilization. While DNS of turbulent premixed flames using realistic chemistry is still restricted to very simple geometries, classical RANS modeling of reacting flows is often considered to lack precision, especially when highly-unsteady problems are considered.

Different methods have been suggested to model turbulent premixed combustion in LES (Colin 2000; Kim & Menon 2000; Duchamp de Lageneste & Pitsch 2000). An approach based on a mixed level-set/diffusion-flamelet library applicable to premixed and partially-premixed combustion has been derived by Peters (1999) for RANS and validated by Herrmann (2000) showing good agreement with experimental data. Beside the fact that this method does not require solving any additional species transport equations or explicit modeling of chemical reaction rates, it also allows the use of arbitrarily complex chemistry without leading to prohibitive computational requirements.

The work presented here focuses on the implementation and validation of a similar approach in the LES context. First, the governing equations to be solved are presented together with the sub-grid models used, including an improved model for the turbulent burning velocity. Then we discuss the application of this approach to two different test cases; a turbulent Bunsen flame (Aachen flame F_3, (Chen 1996) and a lean, partially-premixed dump combustor, the so-called ORACLES geometry described in Besson (1999*a*) and Besson (1999*b*).

2. Governing equations

2.1. *Navier-Stokes equations*

We consider the low-Mach-number approximation to the Navier-Stokes equations (Williams 1985). In the LES context, these equations are written for the filtered variables $\overline{\rho}$, $\widetilde{\mathbf{u}}$ and $\overline{P}$ as:

Mass conservation

$$\frac{\partial \overline{\rho}}{\partial t} + \nabla \cdot (\overline{\rho}\widetilde{\mathbf{u}}) = 0\,, \tag{2.1}$$

Momentum conservation

$$\frac{\partial \overline{\rho}\widetilde{\mathbf{u}}}{\partial t} + \nabla \cdot (\overline{\rho}\widetilde{\mathbf{u}}\widetilde{\mathbf{u}}) = -\nabla \overline{P} + \nabla \cdot (\mu + \mu_t)\widetilde{\tau}\,, \tag{2.2}$$

where the Favre-filtered velocity vector is defined as $\widetilde{\mathbf{u}} = \overline{\rho\mathbf{u}}/\overline{\rho}$, $\widetilde{\tau}$ is the Reynolds stress tensor, and μ_t the turbulent sub-grid eddy viscosity, modeled using a dynamic approach (Moin 1991).

2.2. *G-equation*

In the level-set framework, the instantaneous flame-front location is given by an iso-surface G_0 of a continuous field G. The evolution of this iso-surface is described by the so-called G-equation (Kerstein 1988), valid only at G_0:

$$\frac{\partial G}{\partial t} + \mathbf{u} \cdot \nabla G = s_L |\nabla G|\,, \tag{2.3}$$

where s_L is the laminar burning velocity.

In the context of RANS, Peters (1999) has derived a model equation for the evolution of the mean flame-front location, valid in the corrugated flamelet and the thin reaction zones regime. Keeping in mind that in LES the reaction zone is still much smaller than the grid size, one can see that similar arguments can be used to propose a model equation describing the evolution of the filtered flame-front position. This equation reads

$$\overline{\rho}\frac{\partial \widetilde{G}}{\partial t} + \overline{\rho}\widetilde{\mathbf{u}} \cdot \nabla \widetilde{G} = \underbrace{\overline{\rho} s_T |\nabla \widetilde{G}|}_{Propagation} - \underbrace{\overline{\rho} D_t^G \widetilde{\kappa} |\nabla \widetilde{G}|}_{Curvature}, \tag{2.4}$$

where the turbulent burning velocity s_T as well as the scalar turbulent diffusivity D_t^G have to be modeled.

While a dynamic procedure (Moin 1991; Pierce & Moin 1998) is used to compute D_t^G, the turbulent burning velocity s_T requires further attention.

Peters (1999) derived the following model for s_T, which in addition to the turbulent velocity scales (u'/s_L) also takes the turbulent length scales (Δ_t/l_F) into account.

$$\frac{s_T - s_L}{s_L} = -\frac{a_4 b_3^2}{2b_1}\frac{\Delta_t}{l_F} + \left[\left(\frac{a_4 b_3^2}{2b_1}\frac{\Delta_t}{l_F}\right)^2 + a_4 b_3^2 \frac{u'\Delta_t}{s_L l_F}\right]^{\frac{1}{2}}, \tag{2.5}$$

where Δ_t is the turbulent integral length scale, l_F the laminar flame thickness, u' the turbulent velocity fluctuation and a_4, b_1, and b_3 are constants given in Peters (1999).

A similar expression can be proposed to model s_T in LES where Δ_t then stands for the filter size and u' is the sub-grid velocity fluctuation. The coefficients a_4, b_1, and b_3 also have to be adapted to LES.

As a first approximation, the results reported in Duchamp de Lageneste & Pitsch (2000) were obtained with b_1 and b_3 taken to be the RANS values while a_4 was re-evaluated to be 1.37. This new value was based on a turbulent sub-grid Schmidt number $\mathrm{Sc_t} = 0.4$ instead of 0.7 for RANS, as reported for a non-reacting scalar in a diffusion flame by Pitsch & Steiner (2000). Nevertheless, there is no evidence that the turbulent Schmidt number should remain constant in the case of the scalar $\widetilde{G}$. Consequently, this parameter is now computed locally as $a_4 = D_t^G/(u'\Delta_t)$ where u' and D_t^G are evaluated with a dynamic model.

As a final remark, it is important to note that in order to maintain sufficient regularity

for $\widetilde{G}$, a reinitialization procedure that constrains the $\widetilde{G}$ field to a distance function (such that $|\nabla\widetilde{G}| = 1$) has been implemented (Sethian 1996; Sussman & Fatemi 1999; Russo & Smereka 2000). A detailed description of the implementation of this method in our context can be found in Duchamp de Lageneste & Pitsch (2000).

2.3. *Temperature equation*

In the case of constant molecular properties, only the filtered density is needed in order to solve Eqs. (2.1) and (2.2). Nevertheless, if turbulent heat transport in the unburnt mixture is to be considered, it is necessary to introduce an equation for the filtered temperature $\widetilde{T}$:

$$\overline{\rho}\frac{\partial\widetilde{T}}{\partial t} + \overline{\rho}\widetilde{\mathbf{u}}\cdot\nabla\widetilde{T} = \nabla\cdot(\overline{\rho}D_t^T\nabla\widetilde{T}) + \overline{\rho}\widetilde{\omega}\,, \tag{2.6}$$

where D_t^T is the turbulent diffusivity of the temperature, obtained with a dynamic procedure. Here, $\widetilde{\omega}$ is not a chemical source term, but a volumetric heat source that is used to set $\widetilde{T}$ to the predicted flamelet library value in the burned gases.

Once the filtered temperature is known, the filtered density is recovered via the equation of state.

2.4. *Mixture fraction*

Modeling partial pre-mixing or dilution effects requires the introduction of a conserved scalar $\widetilde{Z}$, similar to the mixture fraction in non-premixed combustion. The burnt temperature is then pre-computed as a function of $\widetilde{Z}$ and its variance $\widetilde{Z''^2}$ by assuming a β-function pdf for this scalar.

In our case the values of $\widetilde{Z}$ range from 0 in pure air to 1 for a stoichiometric mixture, and are given by the solution of

$$\overline{\rho}\frac{\partial\widetilde{Z}}{\partial t} + \overline{\rho}\widetilde{\mathbf{u}}\cdot\nabla\widetilde{Z} = \nabla\cdot(\overline{\rho}D_t^Z\nabla\widetilde{Z})\,, \tag{2.7}$$

where D_t^Z is also computed dynamically.

In partially-premixed cases, where $\widetilde{Z}$ is fluctuating along the G_0 surface, one also has to compute the laminar burning velocity s_L and laminar flame thickness l_F appearing in Eq. (2.5) as functions of $\widetilde{Z}$.

2.5. *Total enthalpy*

If non-adiabatic effects, such as heat losses at boundaries, are to be included, one can also introduce the total enthalpy $\widetilde{H}$ as an additional parameter in the flamelet library. $\widetilde{H}$ is also a conserved scalar and obeys an equation similar to Eq. (2.7). In that case, one of the energy equations, total enthalpy or temperature, would actually be redundant. However, the enthalpy is only used in the burnt gas to determine the burnt temperature from the flamelet library. The volumetric heat source term in Eq. (2.6) is then used to enforce this temperature in the solution of the temperature equation which is then mainly used to describe the turbulent temperature transport in the unburnt gas.

2.6. *Numerical methods*

The code that was used in this study was developed at the Center for Turbulence Research by Pierce & Moin (1998). The filtered low-Mach-number approximation of the Navier-Stokes equations is solved in cylindrical or Cartesian coordinates on a structured staggered mesh that can be refined independently in the axial and radial directions. The

numerical method is a conservative, second-order finite-volume scheme. Second-order semi-implicit time advancement is used, which alleviates the CFL restriction in regions where the grid is refined. Details of the method can be found in Akselvoll & Moin (1996). The code has been thoroughly validated in various studies (Akselvoll 1996; Pierce & Moin 1998, 2001).

3. Large eddy simulation of a turbulent Bunsen flame

The experimental setup studied by Chen (1996) consists of a stoichiometric premixed methane-air flame, stabilized by a large pilot flame. Both incoming streams, the main jet and the pilot, have the same composition. The nozzle diameter D of the main stream is 12 mm. The pilot stream issues through a perforated plate (1175 holes of 1 mm in diameter) around the central nozzle, with an outer diameter of $5.67D$. The main stream is turbulent with a Reynolds number of $\mathrm{Re} = 23486$, based on the inner nozzle diameter and a bulk velocity of $U_0 = 30\,\mathrm{m/s}$.

3.1. *Grid and boundary conditions*

The computational domain extends to $20\,D$ downstream of the nozzle and $4\,D$ in the radial direction. The LES grid is $256 \times 96 \times 64$ corresponding to approximately 1.6 million cells. At the inflow boundary, instantaneous velocities extracted from a separate LES of a fully developed pipe flow are prescribed. Convective conditions (- Akselvoll & Moin 1996) are prescribed at the outflow boundary, while traction-free conditions (Boersma 1998) are imposed on the lateral boundary in order to allow entrainment of fluid into the domain.

3.2. *Results and discussion*

The mean radial profiles of temperature and axial velocity are shown in Fig. 1 for two different downstream locations: here $\overline{\theta}$ is the time-averaged non-dimensional temperature defined by $\overline{\theta} = \left(\overline{T} - T_u\right) / \left(T_b - T_u\right)$, and T_b and T_u are the adiabatic burned and unburned temperatures respectively. $\overline{U}_{ax}$ is the time-averaged axial velocity normalized by the bulk velocity U_0.

Comparison is made between experimental data (denoted by symbols), the LES results reported in Duchamp de Lageneste & Pitsch (2000) (dashed lines) and the actual simulation (solid lines).

The major discrepancies found between the results reported in Duchamp de Lageneste & Pitsch (2000) and the experimental data concerned an over-prediction of the mean temperature increase, leading to an over-prediction of the mean spreading rate of the jet. Chen (1996) noted that, while still in equilibrium, the gases in the pilot flame were found to be at a much lower temperature than the adiabatic temperature, due to heat losses to the burner surface. These heat losses were not taken into account in our previous simulation, and are now modeled by solving a transport equation for the total enthalpy, which appears as a parameter in the flamelet library. Prescribing a lower enthalpy in the pilot stream than in the main jet leads to a predicted maximum value of the mean temperature in good agreement with the experimental data, especially close to the burner (as shown in Fig. 1). As a consequence, the jet expansion due to heat release is now predicted with good accuracy.

While the evolution of the turbulent kinetic energy near the axis was generally well predicted in Duchamp de Lageneste & Pitsch (2000), the maximum value was over-predicted and the location of the peak was shifted toward the burnt side of the flame

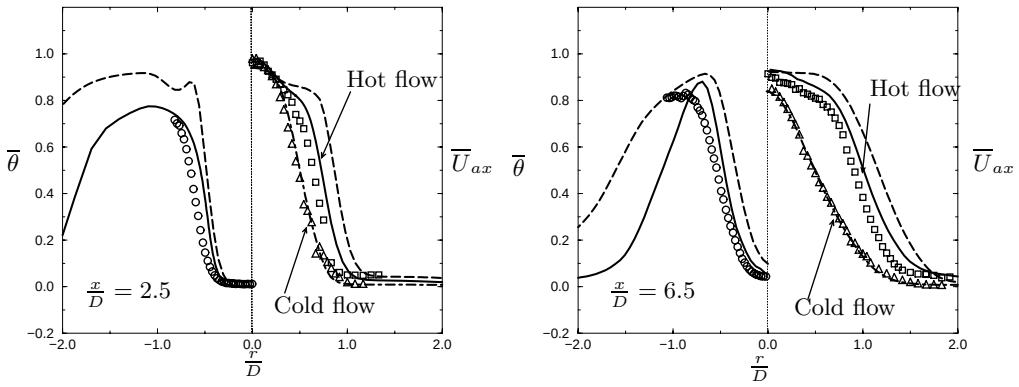

FIGURE 1. Radial profiles of the mean temperature and axial velocity at different axial positions. Symbols represent experimental data, lines LES results. Solid lines: non-adiabatic conditions, dashed lines: adiabatic conditions.

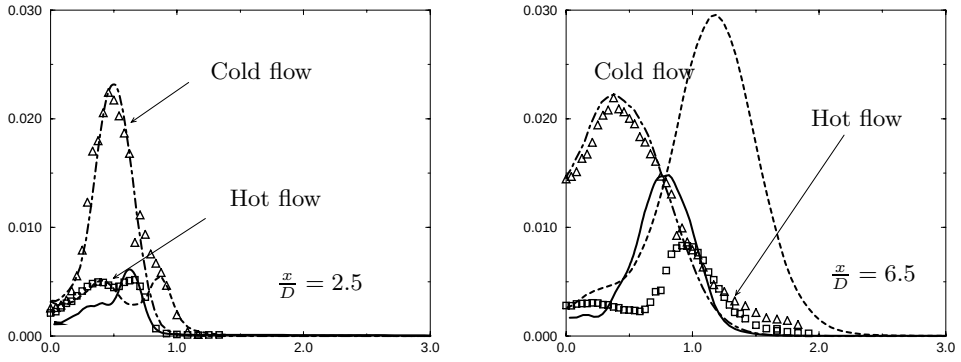

FIGURE 2. Radial profiles of the mean turbulent kinetic energy at different axial locations. Symbols represent experimental data, lines LES results. Solid lines: non-adiabatic conditions, dashed lines: adiabatic conditions.

(dashed lines in Fig. 2). The present simulation shows a clear improvement in both respects. At $x/D = 2.5$, both the location and the value of the peak are well predicted. At $x/D = 6.5$ the peak is well located and even though its value is still somewhat overestimated the agreement with the experimental data is considerably improved.

The intensity of the peak in turbulent kinetic energy located on the burnt side of the flame can be directly related to the development of the mixing layer between the hot burnt gases and the cold entrained air. From this viewpoint, the overestimation of the turbulent kinetic energy in Duchamp de Lageneste & Pitsch (2000), which they found to be growing with distance from the burner, is consistent with the overestimation of the burnt-gas temperature reported in that study. The non-adiabatic conditions used in the present simulation improve the prediction of the location of the heat release, and thereby lead to a much better estimation of the development of the mixing layer. Thus, the slight

over-prediction still observed in the temperature profiles further downstream could be responsible for the higher turbulence intensities found at these locations.

4. Large-eddy simulation of a lean, partially-premixed dump combustor

Constructed at the Laboratoire de Combustion et de Détonique (LCD) de l'ENSMA Poitiers (France) within the Brite-Euram project BE95-1953 (Besson 1999*b*), the test-rig ORACLES has been especially designed to provide accurate experimental data to assess the quality of different approaches in LES of turbulent premixed and partially-premixed combustion.

The experimental setup consists of two channel flows emerging into a wider combustion chamber which is shown in Fig. 3. For the reacting case, the flame is stabilized by the recirculation zones created behind each step. The channels are separated by a splitter plate which is recessed with respect to the expansion to avoid possible anchoring of the flame at the tip of the plate.

Special attention has been paid to providing suitable boundary conditions for LES. The two incoming channels are long enough ($\approx 100\,H$ where H is the step height) to ensure a fully-developed turbulent flow in each stream. In all the cases considered here, the mass flow rate is the same in both channels.

Several different cases have been studied experimentally (Besson 1999*a*). Here we will focus on two of these: the inert flow, used as a reference case, and a reacting case, where the equivalence ratio for the upper stream is 0.9, while it is 0.3 for the lower stream. The main reason for choosing the latter case is that it will provide the opportunity to test the ability of our method to handle partially-premixed turbulent combustion. It is also worth noting that the strong acoustic instabilities that have been detected in most cases with constant equivalence ratio are a problem which has been avoided here, to provide a basic validation of the combustion model.

4.1. *Grid and boundary conditions*

The computational domain extends to $20\,H$ downstream and $4\,H$ upstream of the expansion. The LES grid is $256 \times 128 \times 64$, corresponding to approximately 2.2 million cells. At the inflow boundary, instantaneous velocities obtained from a separate LES of two fully-developed channel flows are prescribed. Convective conditions (Akselvoll & Moin 1996) are used at the outflow boundary while adiabatic no-slip conditions are enforced on all walls.

4.2. *Results and discussion*

4.2.1. *Inert flow*

The basic features of inert flows behind a sudden expansion have been extensively studied both experimentally and numerically (Abbot & Kline 1962; Gagnon 1993).

For the major part of these studies, only one stream is considered, and Abbot & Kline (1962) have shown that the mean flow after a sudden expansion is asymmetrical if the ratio $A_r = (H_{\text{channel}} + 2H_{\text{step}})/H_{\text{channel}}$ is greater than 1.5. For the present case, the area expansion ratio can be evaluated to be $A_r = 1.84$, predicting an asymmetrical mean flow. The experimental results corroborate this prediction, showing an upper mean recirculation zone much shorter than the lower one.

This important feature of the mean flow is captured by the LES, as can be seen on Fig. 3. Furthermore, Fig. 4 shows a comparison of the mean velocity profiles obtained at

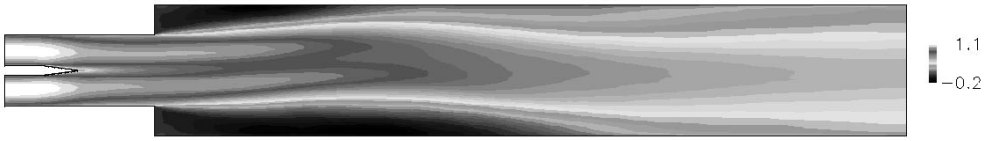

FIGURE 3. Cold flow simulation. Mean axial velocity.

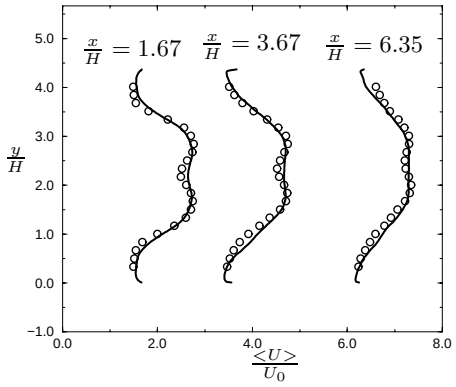

FIGURE 4. Cross-stream profiles of the mean axial velocity at different axial positions for the cold flow case. Symbols represent experimental data, lines LES results.

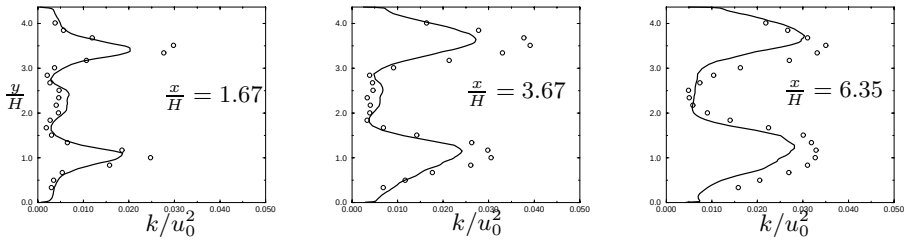

FIGURE 5. Cross-stream profiles of the mean turbulent kinetic energy at different axial positions for the cold flow case. Symbols represent experimental data, lines LES results.

different downstream locations in the inert case and confirms the very good quantitative agreement between the LES results and the experimental data.

Figure 5 shows vertical profiles of the turbulent kinetic energy for the axial positions shown in Fig. 4. The location and width of the peaks of turbulent kinetic energy downstream of each step are precisely predicted by the LES while the maximum intensity is slightly underestimated for the first stations. It can also be observed that the evolution of the local maximum around the symmetry axis created by the mixing layer between the two incoming streams is very well captured.

Since the intensity of the turbulent kinetic energy generated by the central mixing layer

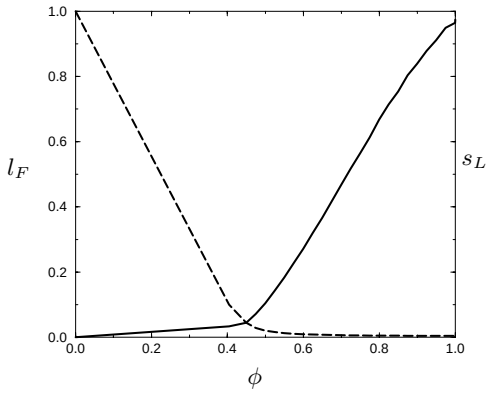

FIGURE 6. s_L (solid line) and l_F (dashed line) as functions of the equivalence ratio ϕ. Both are normalized by their maximum values.

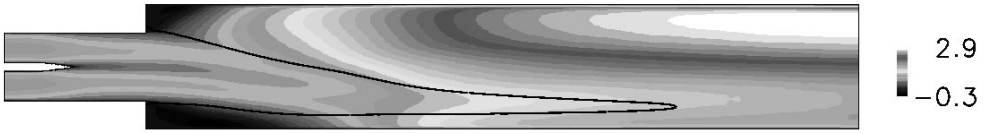

FIGURE 7. Reacting case. Contours of mean axial velocity and of G_0.

is much lower than in the shear layers behind the steps, its influence on the stabilization of the flame can be expected to be small in the reacting case.

4.2.2. *Reacting flow*

In the cold-flow simulation, both inlet channels have the same chemical composition. For the reacting case, the upper channel has a mixture of propane and air at an equivalence ratio of $\phi_1 = 0.9$, while the equivalence ratio in the lower channel is $\phi_2 = 0.3$.

As ϕ will vary along the $\widetilde{G}_0$ surface, the laminar burning velocity s_L and the laminar flame thickness l_F appearing in Eq. (2.5) are now parameterized by ϕ. This dependence is shown in Fig. 6.

As can be seen in Fig. 6, the laminar burning velocity for $\phi = 0.3$ is much lower than for $\phi = 0.9$, while the laminar flame thickness follows the opposite trend. Consequently, the leanest branch of the flame can be expected to be close to the blow-off limit.

Indeed, the preliminary results reported below indicate that the leanest part of the flame barely propagates behind the lower step while the richest part propagates much faster, as shown in Fig. 7. Compared to the cold-flow case shown in Fig. 3, the reacting case exhibits a much shorter upper recirculation zone, due to the strong acceleration behind the richest flame branch. The lower recirculation zone is also shortened, but to a lesser extent.

Figure 8 shows the mean axial velocity profiles obtained at three different locations in the combustion chamber. The velocity increase in the upper part of the chamber due

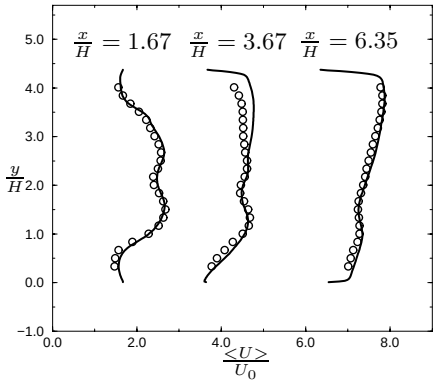

FIGURE 8. Cross-stream profiles of the mean axial velocity at different axial positions for the reacting flow case. Symbols represent experimental data, lines LES results.

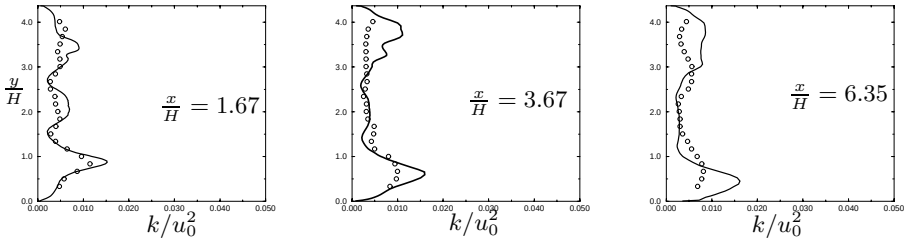

FIGURE 9. Cross-stream profiles of the mean turbulent kinetic energy at different axial positions for the reacting flow case. Symbols represent experimental data, lines LES results.

to heat release is well predicted except for a slight overestimation at $x/H = 3.67$. The corresponding profiles behind the lower step are also different from the cold-flow case. The mean velocity is increased moderately at $x/H = 3.67$, and even more at $x/H = 6.35$. Overall, the quantitative agreement with the experimental data is good.

Finally, Fig. 9 shows vertical profiles of turbulent kinetic energy for the same three axial locations. The agreement is reasonable for all three locations. However the simulation becomes less accurate for the downstream locations, which may indicate that the statistics are not fully converged. Nevertheless, the general trend of diminishing turbulent kinetic energy, especially in the richest part of the flame, is well reproduced. This is in contrast with the cold-flow case where, because of the converging shear layers, the turbulent kinetic energy increases with distance from the steps. In the reacting case, the strong heat release in the upper half of the domain prevents the upper shear layer frm spreading, while the smaller heat release in the bottom half is still sufficient to damp the turbulent fluctuations.

5. Conclusions and future plans

A mixed level-set/flamelet library formulation has been implemented as a suitable model for large-eddy simulation of turbulent premixed and partially-premixed flames.

The versatility of this approach has been demonstrated through its application to two very different cases.

The first study concerns the Aachen flame F_3, where the model has been shown to yield predictions in good agreement with the experimental data of Chen (1996). Two different simulations have been performed for this case. The first simulation uses adiabatic conditions. In the second approach, the total enthalpy is used as a parameter in the flamelet library to take heat losses near the burner exit into account. The latter refined model shows improved accuracy through a better physical description, with only a small computational overhead.

The second study presented in this report concerns the LES of a turbulent, partially-premixed lean dump combustor, the so-called ORACLES burner. Results are compared to the experimental data of Besson (1999*a*) for the non-reacting and reacting cases. The non-reacting case was found to exhibit recirculation zones which are asymmetric in the mean, typical of supercritical flows through sudden expansions. This behavior is well recovered by the LES, both qualitatively and quantitatively. The turbulent kinetic energy is also predicted with reasonable accuracy. Preliminary results for the reacting case are also presented showing very good agreement with experimental data for the time-averaged axial velocity. The turbulent kinetic energy is predicted less accurately than in the non-reacting case, although the overall agreement remains acceptable.

In the future we will focus on the derivation of a dynamic model for the turbulent burning velocity that will be tested against the present algebraic model. In addition the model will be applied to other ORACLES cases revealing combustion instabilities.

Acknowledgments

This work was supported in part by SNECMA Motors and the Department of Energy within the ASCI program.

REFERENCES

Abbot, D. E. & Kline, S. J. 1962 Experimental investigation of a subsonic turbulent flow over a single and double backward facing steps. *J. Basic Engg.* **84**, 317–325.

Akselvoll, K. 1996 An efficient method for temporal integration of the navier-stokes equations in confined axisymmetric geometrie. *J. Comp. Phys.* **125**, 454–463.

Akselvoll, K. & Moin, P. 1996 Large-eddy simulation of turbulent confined co-annular jets. *J. Fluid Mech.* **31**, 387–411.

Besson, M., Bruel, P., Champion, J. L. & Deshaies, B. 1999*a* Inert and combusting flows developping over a plane symmetric expansion: experimental analysis of the main flow characteristics. In *AIAA* paper 99-0412.

Besson, M., Bruel, P. & Deshaies, B. 1999*b* The contribution of ENSMA. Final Technical Report. *Tech. Rep.* BRITE EURAM-AERO BE95-1953.

Boersma, B., Brethouwer, G. & Nieuwsdat, F. T. 1998 A numerical investigation on the effect of the inflow conditions on the self-similar region of a round jet. *Phys. Fluids* **10**, 899–909.

Chen, Y. C., Peters, N., Schneemann, G. A., Wruck, N., Renz, U. & Mansour,

M. S. 1996 The detailed flame structure of highly stretched turbulent premixed methane-air flames. *Comb. and Flame* **107**, 233–244.

Colin, F., Veynante, D. & Poinsot, T. 2000 A thickened flame model for large eddy simulation of premixed turbulent combustion. *Phys. Fluids* **12**, 1843–1863.

Gagnon, Y., Giovannini, A. & Hébrard, P. 1993 Numerical simulation and physical analysis of high reynolds number recirculating flows behind sudden expansions. *Phys. Fluids* **5**, 2377–2389.

Herrmann, M. 2000 Numerische Simulation vorgemischter und teilweise vorgemischter Turbulenten Flamen. PhD thesis, RWTH, Aachen.

Kerstein, A. R., Ashurst, W. T. & Williams, F. A. 1988 Equation for interface propagation in an unsteady homogeneous flow field. *Phys. Rev. A* **37**, 2728–2731.

Kim, W. W. & Menon, S. 2000 Numerical modeling of turbulent premixed flames in the thin-reaction zones regime. *Comb. Sci. Tech.* **26**, 1–32.

Duchamp de Lageneste, L. & Pitsch, H. 2000 A level-set approach to large eddy simulation of premixed turbulent combustion. *Annual Research Briefs*, Center for Turbulence Research, NASA Ames/Stanford Univ. 105–116.

Moin, P., Squires, K., Cabot, W. & Lee, S. 1991 A dynamic subgrid-scale model for compressible turbulence and scalar transport. *Phys. Fluids* **A**, 2746–2757.

Muniz, L. & Mungal, G. 1997 Instantaneous flame stabilization velocities in lifted-jet diffusion flames. *Comb. and Flame* **111**, 16–31.

Nilsson, P. & Bai, X. S. 2000 Level-set flamelet library approach for premixed turbulent combustion. *Env. Therm. Fluid Sci.* **21**, 87–98.

Peters, N. 1999 Turbulent burning velocity for large-scale and small-scale turbulence. *J. Fluid Mech.* **384**, 107–132.

Peters, N. 2000 *Turbulent Combustion*. Cambridge University Pres.

Pierce, C. D. & Moin, P. 1998 Large eddy simulation of a confined jet with swirl and heat release. In *AIAA P.*, vol. 98-2892.

Pierce, C. D. & Moin, P. 2001 Progress-variable approach for large eddy simulation of turbulent combustion. *Tech. Rep.* TF-80. Dept. Mech. Eng., Stanford University.

Pitsch, H. & Steiner, H. 2000 Large eddy simulation of a turbulent piloted methane/air diffusion flame. *Phys. Fluids* **12**, 2541–2553.

Russo, G. & Smereka, P. 2000 A remark on computing distance functions. *J. Comp. Phys.* **163**, 51–67.

Sethian, J. A. 1996 *Level Set Methods : Evolving Interfaces in Geometry, Fluid Mechanics, Computer Vision and Material Science*. Cambridge University Press.

Su, L. K., Han, D. & Mungal, G. 2000 Experimental results on the stabilization of lifted jet diffusion flames. *Annual Research Briefs*, Center for Turbulence Research, NASA Ames/Stanford Univ. 79–89.

Sussman, M. & Fatemi, E. 1999 An efficient, interface-preserving level set re-distancing algorithm and its application to interfacial incompressible fluid flow. *SIAM Journ. Sci. Comp.* **20**, 1165–1191.

Veynante, D., Vervisch, L., Poinsot, T., Liñan, A. & Ruetsch, G. R. 1994 Triple flame structure and diffusion flame stabilization. *Proc. Summer Program*, Center for Turbulence Research, NASA Ames/Stanford Univ. 55–73.

Williams, F. A. 1985 Turbulent combustion. In *Math. of Comb.*, (J. Buckmaster, Ed.) 97–131.